HYPER VERSION

RECEIVED: *January 1, 0000,* ACCEPTED: *January 1, 0000*
REVISED: *January 1, 0000*

JHEP00(0000)000

Signatures of photon and axion-like particle mixing in the gamma-ray burst jet

Olga Mena,[a] **Soebur Razzaque,**[b,*] **and F. Villaescusa-Navarro**[a]

[a] *IFIC, Universidad de Valencia-CSIC, E-46071, Valencia, Spain*
[b] *College of Science, George Mason University, Fairfax, Virginia 22030, USA*
E-mail: omena@ific.uv.es, srazzaqu@gmu.edu, francisco.Villaescusa@ific.uv.es

ABSTRACT: Photons couple to Axion-Like Particles (ALPs) or more generally to any pseudo Nambu-Goldstone boson in the presence of an external electromagnetic field. Mixing between photons and ALPs in the strong magnetic field of a Gamma-Ray Burst (GRB) jet during the prompt emission phase can leave observable imprints on the gamma-ray polarization and spectrum. Mixing in the intergalactic medium is not expected to modify these signatures for ALP mass $> 10^{-14}$ eV and/or for $<$ nG magnetic field. We show that the depletion of photons due to conversion to ALPs changes the linear degree of polarization from the values predicted by the synchrotron model of gamma ray emission. We also show that when the magnetic field orientation in the propagation region is perpendicular to the field orientation in the production region, the observed synchrotron spectrum becomes steeper than the theoretical prediction and as detected in a sizable fraction of GRB sample. Detection of the correlated polarization and spectral signatures from these steep-spectrum GRBs by gamma-ray polarimeters can be a very powerful probe to discover ALPs. Measurement of gamma-ray polarization from GRBs in general, with high statistics, can also be useful to search for ALPs.

KEYWORDS: axions, gamma ray bursts theory, magnetic fields, gamma ray burst experiments.

*Present address: Naval Research Laboratory, Washington, DC 20375, USA

Contents

1. Introduction

Axions represent the most convincing and elegant solution to the strong CP problem [1]. They are the pseudo Nambu-Goldstone bosons of a global $U(1)_{PQ}$ symmetry [2, 3]. Axion-Like Particles (ALPs) can be understood as generalizations of the axions, and appear generally in theories beyond the Standard Model (SM) of Particle Physics. Axions and ALPs couple to photons in the presence of an external electromagnetic field [4]. For axions the strength of the coupling $g_{a\gamma}$ is inversely proportional to the energy scale M at which the $U(1)_{PQ}$ symmetry is spontaneously broken, and is directly related to the particle mass m_a. For ALPs there is no general relation between the energy scale of the new physics beyond the SM and the ALP mass, and therefore in the following we shall consider the parameters $g_{a\gamma}$ and m_a to be independent of each other. ALPs may be copiously produced in the early universe, either thermally [5] or non-thermally [6], providing a possible (sub) dominant (hot) dark matter candidate.

Mixing of photons and ALPs in an electromagnetic field results in photon-ALP conversion and a change in photon polarization states. The former effect has been extensively exploited to search for ALPs that are created in the Sun, travel to the Earth as ALPs and convert to $\sim$ keV photons in the magnetic field of a laboratory experiment. From non-detection of such photons, the CAST experiment has reported a lower bound on the ALP energy scale of $M > 1.1 \cdot 10^{10}$ GeV, which translates to a constraint on the photon-ALP coupling of $g_{a\gamma} < 8.8 \cdot 10^{-11}$ GeV^{-1} for ALP masses of $m_a \sim 0.02$ eV [7]. These constraints exclude a region in the $g_{a\gamma}$–m_a parameter space. The same conversion mechanism is used by the ADMX experiment to search for ALP dark matter that converts to microwave photons [8].

Observation of supernovae (SNe) Ia dimming has been suggested as a possible signature of photon-to-ALP conversion, thus depleting the photon flux, in the Inter-Galactic

Magnetic Field (IGMF) [9, 10, 11, 12, 13, 14]. This is an alternative to the standard interpretation by a dark energy fluid that is responsible for recent accelerated expansion of the Universe, making the distances of the SNe Ia larger. Search for circular polarization in the Cosmic Microwave Background (CMB) data has been proposed as probe of photon-ALP mixing in the IGMF [15]. Mixing in the IGMF has also been considered as a possible mechanism to produce ultra-high energy cosmic-ray events, assumed to be photons which are not attenuated while in their ALP states and while propagating from distant sources to the Earth [16]. A similar mechanism has been proposed to search for photon-ALP conversion effects in the GeV–TeV γ-ray fluxes from distant active galactic nuclei [17, 18, 19, 20]. Detection of these fluxes at very high energies may provide hints of photon-ALP mixing, which would be absorbed by the Extragalactic Background Light (EBL) otherwise (see e.g. Ref. [21]).

Here we study the observational consequences of a photon-ALP coupling on GRB photon polarization and fluxes at *low energies*, in the $\sim$ keV–MeV range, arising from high magnetic field in the GRB jet. [1] A search in this energy range has several advantages: (i) GRBs, the most powerful explosions in the Universe, release upwards of 10^{53} erg of isotropic-equivalent γ-ray energy, mostly in the $\sim$ keV–MeV range [25]. Thus we have the most powerful photon beam at our disposal to investigate the effect. (ii) Unlike TeV γ rays, MeV photons are not attenuated in the EBL and detection of any effect due to photon-ALP coupling does not depend on the EBL models (see e.g. Refs. [26, 27, 28, 29, 30]). (iii) Since photons are converted to ALPs in the high magnetic field of the GRB jet, ALPs may not convert back to photons while propagating in the IGMF and in the galactic magnetic fields[2] . Search for photon-ALP mixing in the photon polarization data has been suggested for GRBs in the past, both in the strong magnetic field of the GRB [31] and in the IGMF [32] (see also Ref. [33]). We have studied effects of photon-ALP mixing on GRB γ-ray polarization using a realistic emission model, namely synchrotron radiation by relativistic electrons in the strong magnetic field, either advected from the GRB central engine [34, 35] or generated in the shocks [36, 37, 38, 39] or both.

In the synchrotron model, which is also the leading model for observed $\sim$ keV–MeV γ-ray emission, a population of electrons are assumed to be injected as a power-law above a minimum particle Lorentz factor in the magnetized plasma with an optical depth less than unity. The peak of the observed energy spectrum ($E^2\,dN/dE$), typically in the $\sim$ 0.1–1 MeV range, is identified with the characteristic synchrotron frequency from the electrons with the minimum Lorentz factor in the comoving GRB jet frame, boosted by the bulk Lorentz factor of the jet. Synchrotron radiation is partially polarized with a linear polarization degree of $\approx$ 50% at frequencies much lower than the characteristic frequency, reaching $\approx$ 70% at the maximum [40]. We model the initial polarization states of the observed photons in the $\sim$ keV–MeV γ rays as from the electrons with minimum Lorentz factor, according to synchrotron radiation theory in the comoving frame. The effect of photon-

[1] GRB pseudo-Goldstone boson emission and its subsequent conversion to electromagnetic energy was proposed as a possible mechanism for the observed GRBs [22, 23, 24]. We do not address such a possibility in the present study.

[2] They can, however, convert back to photons in a suitable laboratory experiment.

ALP mixing then changes the observed polarization from the expected pattern.

To date, prompt γ ray polarization has been measured from only a handful of GRBs, most notably an $(80 \pm 20)\%$ linear polarization from GRB 021206 by *RHESSI* [41]. However, these measurements are statistically inconclusive and suffer from large systematic uncertainties (see e.g. Ref. [42]). Gamma-Ray Burst Polarimeter (GAP), sensitive in the 50–300 keV range, aboard the recently launched *IKAROS Solar Sail* is one of the new generation of instruments to measure γ ray polarization [43]. A number of satellite missions such as the Advanced Compton Telescope (ACT) [44], Gamma-ray Burst Investigation via Polarimetry and Spectroscopy (GRIPS) [45], and Polarimeters for Energetic Transients (POET) [46] are also being planned to measure γ ray polarization in the keV–MeV range. These experiments are expected to measure GRB polarization with a high statistical significance and have been shown to be excellent tools to test the synchrotron emission models (see e.g. Ref. [47]). Eventually, these broadband polarimeters will be able to detect deviations from the standard synchrotron polarization pattern. Such frequency-dependent deviations in the polarization pattern could be explained in terms of photon-ALP mixing.

The polarization pattern induced by photon-ALP mixing can be accompanied with a detectable change in the γ-ray spectral slope, due to a depletion of preferentially low energy photons that convert to ALPs in the GRB jet. Indeed a specific prediction of the GRB synchrotron model is that, below the peak energy the spectrum can not be harder than the photon index $\alpha_\gamma = -2/3$, where $dN/dE \propto E^{\alpha_\gamma}$, a limit that arises from synchrotron theory of radiation from a single particle [40, 48]. Observed variation of the GRB low-energy spectra softer than this limit may be explained as cooling effect on the electron spectrum, producing a γ-ray spectrum as soft as $dN/dE \propto E^{-3/2}$ (see, e.g., Ref. [49]). Majority of bright GRBs, detected by the Burst And Transient Source Experiment (BATSE) aboard the *Compton Gamma Ray Observatory*, for which good spectral data are available [50] falls within the synchrotron limit of $-2/3 \geq \alpha_\gamma \geq -3/2$. However a significant ($\sim 20\%$) fraction violates the "synchrotron death line" of $\alpha_\gamma = -2/3$ [51], and a "harder when brighter" tendency is present in the data. The same effect has been detected in time-integrated and time-resolved spectra from joint observations by the Burst Alert Telescope (BAT) aboard *Swift* and by the Wide band All-sky Monitor (WAM) aboard *Suzaku* [52], and most recently by the Gamma-ray Burst Monitor (GBM) aboard the *Fermi Gamma-ray Space Telescope* [53]. We predict that polarization measurements of these steep-spectrum GRBs can shed light, or even lead to discovery of ALPs.

The structure of the paper is as follows. We review the photon-ALP mixing phenomena in Sec. 2 and apply this formalism to the GRB jet and synchrotron emission model in Sec. 3. We discuss our results in Sec. 4 and conclude our study in Sec. 5.

2. Photon-ALP mixing and conversion probabilities

We follow here the photon-axion/ALP interaction formalism from Ref. [4] (see also Ref. [32]).

The lagrangian for the photon-ALP system is given by[3]

$$\mathcal{L} = -\frac{1}{4} F_{\mu\nu} F^{\mu\nu} + \frac{\alpha^2}{90\, m_e^4} \left[(F_{\mu\nu} F^{\mu\nu})^2 + \frac{7}{4} \left(F_{\mu\nu} \tilde{F}^{\mu\nu} \right)^2 \right] + \frac{1}{2} \partial^\mu a \, \partial_\mu a - \frac{1}{2} m_a^2 \, a^2 - \frac{1}{4} g_{a\gamma} F_{\mu\nu} \tilde{F}^{\mu\nu} a \ , \tag{2.1}$$

where $F_{\mu\nu}$ is the electromagnetic field tensor, $\tilde{F}_{\mu\nu} = \frac{1}{2} \epsilon_{\mu\nu\rho\sigma} F^{\rho\sigma}$ is its dual, α is the fine-structure constant and m_e is the electron mass. The second term in Eq. (2.1) is the Euler-Heisenberg effective Lagrangian, which accounts for one-loop corrections to the classical electrodynamics. The third and fourth terms in Eq. (2.1) are the Lagrangian terms describing the ALP field a with a mass m_a. The last term is the photon-ALP interaction lagrangian, which, in terms of the external electromagnetic field, reads

$$\mathcal{L}_{a\gamma} = -\frac{1}{4} g_{a\gamma} F_{\mu\nu} \tilde{F}^{\mu\nu} a = g_{a\gamma} \, \mathbf{E} \cdot \mathbf{B} \, a \ . \tag{2.2}$$

Here $g_{a\gamma}$ is the photon-ALP coupling constant, $\mathbf{E}$ and $\mathbf{B}$ are the electric and magnetic fields respectively.

The evolution equations for a mono-energetic photon/ALP beam with energy ω propagating along the z direction in an external and homogeneous magnetic field transverse ($\mathbf{B}_T$) to the beam direction (i.e. in the x-y plane) are given by:

$$\begin{aligned} \omega^2 A_\perp + \partial_z^2 A_\perp + \frac{4\alpha}{45\pi} \left(\frac{B_T}{B_{\rm crit}} \right)^2 \omega^2 A_\perp - \frac{4\pi n_e \alpha}{m_e} A_\perp &= 0 \ , \\ \omega^2 A_\parallel + \partial_z^2 A_\parallel + \frac{7\alpha}{45\pi} \left(\frac{B_T}{B_{\rm crit}} \right)^2 \omega^2 A_\parallel + \omega g_{a\gamma} B_T a - \frac{4\pi n_e \alpha}{m_e} A_\parallel &= 0 \ , \\ \omega^2 a + \partial_z^2 a - m_a^2 a + \omega g_{a\gamma} B_T A_\parallel &= 0 \ . \end{aligned} \tag{2.3}$$

Here $A_\perp$ and $A_\parallel$ are the two photon polarization components (both in the x-y plane) perpendicular and parallel to the external magnetic field $\mathbf{B}_T$, respectively. The plasma term in the equations of motion arises due to the presence of electrons in the media, giving an effective mass to the photons, and is proportional to the electron number density n_e. The critical magnetic field is defined as $B_{\rm crit} \equiv m_e^2/e = 4.414 \cdot 10^{13}$ G, where e is the electron charge. In the limit where $\omega \gg m_a$, the evolution of the system can be linearized in the form of a first order differential equation[4]

$$\left(i \frac{d}{dz} + \omega + \mathcal{M} \right) \begin{pmatrix} A_\perp(z) \\ A_\parallel(z) \\ a(z) \end{pmatrix} = 0 \ . \tag{2.4}$$

Here $\mathcal{M}$ is a mixing matrix of the axion field with the photon polarization components, and is given by

$$\mathcal{M} = \begin{pmatrix} \Delta_\perp & 0 & 0 \\ 0 & \Delta_\parallel & \Delta_{a\gamma} \\ 0 & \Delta_{a\gamma} & \Delta_a \end{pmatrix} \ . \tag{2.5}$$

[3]We adopt the natural unit convention $\hbar = c = 1$.

[4]We follow the notation adopted in Ref. [32].

The elements of $\mathcal{M}$ can be expressed as $\Delta_\perp \equiv 2\Delta_{\rm QED} + \Delta_{\rm pl}$, $\Delta_\parallel \equiv (7/2)\Delta_{\rm QED} + \Delta_{\rm pl}$ following Ref. [32], and we provide their reference values relevant in our case below

$$\begin{aligned}
\Delta_{\rm QED} &\equiv \frac{\alpha\omega}{45\pi}\left(\frac{B_T}{B_{\rm cr}}\right)^2 \simeq 1.34\cdot 10^{-12}\left(\frac{\omega}{\rm keV}\right)\left(\frac{B_T}{10^6\,{\rm G}}\right)^2\ {\rm cm}^{-1},\\
\Delta_{\rm pl} &\equiv -\frac{\omega_{\rm pl}^2}{2\omega} \simeq -3.49\cdot 10^{-12}\left(\frac{\omega}{\rm keV}\right)^{-1}\left(\frac{n_e}{10^8\,{\rm cm}^{-3}}\right)\ {\rm cm}^{-1},\\
\Delta_{a\gamma} &\equiv \frac{1}{2}g_{a\gamma}B_T \simeq 1.32\cdot 10^{-11}\left(\frac{g_{a\gamma}}{8.8\cdot 10^{-11}\,{\rm GeV}^{-1}}\right)\left(\frac{B_T}{10^6\,{\rm G}}\right)\ {\rm cm}^{-1},\\
\Delta_a &\equiv -\frac{m_a^2}{2\omega} \simeq -2.53\cdot 10^{-13}\left(\frac{\omega}{\rm keV}\right)^{-1}\left(\frac{m_a}{10^{-7}\,{\rm eV}}\right)^2\ {\rm cm}^{-1}.
\end{aligned} \tag{2.6}$$

The plasma frequency is defined as $\omega_{\rm pl} = \sqrt{4\pi\alpha n_e/m_e} = 3.71\cdot 10^{-14}\sqrt{n_e/{\rm cm}^{-3}}$ keV. Notice from Eqs. (2.4) and (2.5) that the component of the photon beam polarization perpendicular to the $\mathbf{B}_T$ field, $A_\perp$, will decouple from the evolution of the photon-ALP system. In other words the ALP couples only to the $A_\parallel$ polarization component.

A generalization of the scenario discussed so far is when $\mathbf{B}_T$ makes an angle ξ, $0 \leq \xi \leq 2\pi$, with the y axis in a fixed coordinate system. A rotation of the mixing matrix [Eq. (2.5)] in the x-y plane then leads to a new form and the evolution equation of the photon-ALP system reads

$$i\frac{d}{dz}\begin{pmatrix} A_\perp(z)\\ A_\parallel(z)\\ a(z)\end{pmatrix} = -\begin{pmatrix} \Delta_\perp\cos^2\xi + \Delta_\parallel\sin^2\xi & \cos\xi\sin\xi(\Delta_\parallel - \Delta_\perp) & \Delta_{a\gamma}\sin\xi\\ \cos\xi\sin\xi(\Delta_\parallel - \Delta_\perp) & \Delta_\perp\sin^2\xi + \Delta_\parallel\cos^2\xi & \Delta_{a\gamma}\cos\xi\\ \Delta_{a\gamma}\sin\xi & \Delta_{a\gamma}\cos\xi & \Delta_a\end{pmatrix}\begin{pmatrix} A_\perp(z)\\ A_\parallel(z)\\ a(z)\end{pmatrix}. \tag{2.7}$$

If there are more than one magnetic field domain present in the problem, then Eq. (2.7) needs to be solved for each domain with appropriate initial conditions. Under the assumptions that all the domains in a particular environment (constant n_e and the same initial conditions for the fields at $z = 0$) have identical coherence lengths and magnetic field strengths, and only the orientation of the magnetic field $\mathbf{B}_T$ in each domain is random, then the average effect can be calculated by randomly varying ξ. We mainly consider the scenario where photons are created at $z = 0$, at source, and cross $\mathbf{B}_T$ field domains where (i) $\xi = 0$ or $\pi/2$ in each domain, and (ii) ξ is random. In both cases each photon crosses only one coherence length width in the z direction. The final beam consists of contributions from all domains. This is different from propagation of the beam in the intergalactic medium where each photon/ALP crosses many IGMF domains and the initial conditions change each time the beam enters a domain (see, e.g. Ref. [32]).

In analogy with two-family neutrino mixing, the conversion probability of $A_\parallel$ into ALPs after traveling a coherence length L and for $\xi = 0$ reads

$$P_{a\gamma} = \sin^2 2\theta\sin^2\left(\frac{\Delta_{\rm osc}\,L}{2}\right), \tag{2.8}$$

where the oscillation wave number is $\Delta_{\rm osc} = \sqrt{(\Delta_a - \Delta_\parallel)^2 + 4\Delta_{a\gamma}^2}$ and the mixing angle is $\theta = (1/2)\arctan[2\Delta_{a\gamma}/(\Delta_\parallel - \Delta_a)]$. From Eq. (2.8) it is possible to infer the energy range

in which the conversion probabilities are approximately energy independent and mixing effects will be maximal ($\theta \approx \pi/4$) for $\omega_L \leq \omega \leq \omega_H$, where the low and high critical energies, respectively, are given by [19, 20, 32]

$$\omega_L \equiv \frac{E\,|\Delta_a - \Delta_{\rm pl}|}{2\,\Delta_{a\gamma}} \simeq \frac{0.12\,|m_a^2 - \omega_{\rm pl}^2|}{(10^{-7}{\rm eV})^2} \left(\frac{B_T}{10^6\ {\rm G}}\right)^{-1} \left(\frac{g_{a\gamma}}{8.8\cdot 10^{-11}\ {\rm GeV}^{-1}}\right)^{-1} {\rm keV},$$
$$\omega_H \equiv \frac{90\pi\, g_{a\gamma}\, B_{\rm cr}^2}{7\alpha\, B_T} \simeq 5.62 \left(\frac{B_T}{10^6\ {\rm G}}\right)^{-1} \left(\frac{g_{a\gamma}}{8.8\cdot 10^{-11}\ {\rm GeV}^{-1}}\right) {\rm keV}. \quad (2.9)$$

We focus on the specific problem of photon-ALP mixing in the GRB jet and the impact of the photon-ALP conversions in the observed photon spectrum in the next section.

3. Gamma-ray emission and conversion to ALPs in the GRB jet

Synchrotron radiation from relativistic electrons that are accelerated in the GRB jet, either due to dissipation of the jet kinetic energy (internal shocks of plasma shells) [36] or magnetic flux [34] from a central engine, is believed to be the dominant mechanism to produce observed γ rays in the keV–MeV range. In the internal shocks model the conversion of jet kinetic energy to γ rays takes place at a radius $R \approx 2\Gamma^2 c t_v \sim 2.7{\cdot}10^{13}\ (\Gamma/300)^2 (t_v/10^{-2}\ {\rm s})$ cm, which can vary widely depending on the jet bulk Lorentz factor Γ and the γ ray flux variability time scale t_v. The jet kinetic energy is typically estimated from the observed isotropic-equivalent γ-ray luminosity L_γ and assuming that a fraction ϵ_e of the kinetic energy is converted to relativistic electrons which promptly radiate most of their energy to γ rays. Random magnetic field in the GRB jet is believed to arise when a fraction ϵ_B of the jet kinetic energy is converted to the magnetic field energy in the shocks (see e.g. Ref. [39, 54]). An average value of the magnetic field and electron density can be estimated, in the jet comoving frame, as $B \sim 5\cdot 10^4\,(\epsilon_B/\epsilon_e)^{1/2} (L_\gamma/10^{52}\ {\rm erg\ s^{-1}})^{1/2} (\Gamma/300)^{-3} (t_v/10^{-2}\ {\rm s})^{-1}$ G and $n_e \sim 2\cdot 10^8\,\epsilon_e^{-1} (L_\gamma/10^{52}\ {\rm erg\ s^{-1}}) (\Gamma/300)^{-6} (t_v/10^{-2}\ {\rm s})^{-2}\ {\rm cm^{-3}}$ (see e.g. Ref. [55]).

Strong magnetic field from the central engine can also be present in the GRB jet. The toroidal component of the magnetic field of a magnetar with surface magnetic field B_0 at $R_0 \approx 10^6$ cm drops to a value $B = B_0(R_0/R) \approx 10^8 (B_0/10^{15}\ {\rm G})(R/10^{13}\ {\rm cm})^{-1}$ G at a dissipation radius R. The magnetic field from the central engine is globally ordered in the emission region. The coherence length scale of the random magnetic field can be as small as the plasma skin depth [39, 54], however efficient conversion of the shock energy to γ rays requires a length scale of the order of the comoving width of the plasma shell $\langle \Delta R \rangle \approx \Gamma c t_v \sim 9\cdot 10^{10}\,(\Gamma/300)(t_v/10^{-2}\ {\rm s})$ cm. Because of relativistic beaming, only an angular size scale $1/\Gamma$ of the jet surface is viewable. Note that, this also corresponds to a maximum length scale $\langle \Delta R \rangle$ over which the random magnetic field can be fully ordered due to causality [54]. The jet half-opening angle $\theta_{\rm jet}$ is much larger than $1/\Gamma$ during the prompt γ-ray emitting phase. Both the ordered and random magnetic fields are mostly perpendicular to the jet axis, which is assumed along the z direction.

Synchrotron radiation from the visible patch of the jet surface can reach the maximum polarization degree, $\approx 50\%$–70%, if the magnetic field is fully ordered in the patch and $\Gamma\theta_{\rm jet} \gg 1$. Intrinsic curvature of the field, for example in case of toroidal field configuration,

in a large visible patch can reduce the maximum polarization degree to $\approx 40\%$ [56, 47]. Smaller scale random magnetic field, if dominant, can also reduce the net polarization degree [54, 47]. We explore both the ordered and random field scenarios to calculate photon-ALP mixing in the GRB jet. Moreover, the emission region and propagation region of the photons can be separated with different magnetic field strengths and orientations (i.e. $\xi \neq 0$). Faraday rotation of the polarization plane can be important for synchrotron radiation [40] only for a substantial magnetic field component parallel to the beam direction (along the z axis) and below the optical frequencies, both situations are outside the scope of this paper. Mixing of the $A_\parallel$ and $A_\perp$ components in our scenario takes place through the off-diagonal terms in the mixing matrix [Eq. (2.7)], due to ξ. Additional ordered magnetic field (e.g. in the wind of the progenitor star) surrounding the GRB jet [56], if present and is sufficiently strong, can modify some of the polarization effect that we explore here. However we ignore that for simplicity.

The two photon polarization components in synchrotron radiation can be written in terms of the Bessel functions (see e.g. Ref. [40]) as[5]

$$\begin{aligned} A_\parallel(\omega) &= \frac{\sqrt{3}\gamma_e^2\theta_e}{\omega_c}\sqrt{1+\gamma_e^2\theta_e^2}\, K_{1/3}\left(\frac{\omega}{2\omega_c}\right) , \\ A_\perp(\omega) &= i\frac{\sqrt{3}\gamma_e}{\omega_c}(1+\gamma_e^2\theta_e^2)\, K_{2/3}\left(\frac{\omega}{2\omega_c}\right) , \end{aligned} \tag{3.1}$$

from a single electron with Lorentz factor γ_e gyrating in the $\mathbf{B}$ field. Here θ_e is the angle between the line of sight and the plane containing the electron trajectory. The characteristic synchrotron frequency, in case $\theta_e \to 0$, is given by

$$\omega_c = \frac{3}{2}\frac{B\sin\eta}{B_{\rm crit}}\gamma_e^2 m_e\,, \tag{3.2}$$

where η is the pitch angle between the electron's velocity and $\mathbf{B}$. The intensity of synchrotron radiation is given by

$$\frac{d^2I}{d\omega d\Omega} = \frac{e^2\omega^2}{4\pi^2}\left(|A_\parallel(\omega)|^2 + |A_\perp(\omega)|^2\right) , \tag{3.3}$$

and the emitted radiation is concentrated in a solid angle $d\Omega = 2\pi\sin\eta\, d\theta_e$. The power emitted per unit frequency is calculated by dividing the intensity with the orbital period of the charge, $T = 2\pi\gamma_e m_e/eB$, after integrating over the solid angle as

$$P(\omega) = \frac{e^3\omega^2 B\sin\eta}{4\pi^2\gamma_e m_e}\int\left(|A_\parallel(\omega)|^2 + |A_\perp(\omega)|^2\right) d\theta_e\,. \tag{3.4}$$

The degree of linear polarization for a mono-energetic electron is given by [40]

$$\Pi_L \equiv \frac{P_\perp(\omega) - P_\parallel(\omega)}{P_\perp(\omega) + P_\parallel(\omega)} , \tag{3.5}$$

[5]Note that Ref. [48] uses exactly the opposite convention for the polarization components.

where $P_\perp(\omega)$ and $P_\parallel(\omega)$ are the powers emitted per unit frequency in directions parallel and perpendicular to the magnetic field, and can be calculated from Eq. (3.4).

The total synchrotron power from a distribution of electrons[6] can be calculated by performing the convolution of the power from each electron and by integrating over γ_e. In the keV–MeV range of our interest, however, γ rays from GRBs are modeled as synchrotron radiation from the shock-accelerated electrons of a minimum Lorentz factor $\gamma_{e,m}$. The observed peak photon energy in the $E^2(dN/dE)$ energy spectrum (often denoted as $EF(E)$ or νF_ν) corresponds to the characteristic photon energy in Eq. (3.2), after multiplying by a $\Gamma/(1+z)$ factor, as $E_{\rm pk} \sim 3.5\,(1+z)^{-1}(B\sin\eta/10^6\ {\rm G})(\gamma_{e,m}/10^3)^2\Gamma_{300}$ MeV. The typical GRB redshift is $z \approx$ 1–2. Higher energy photons, but not too far above $E_{\rm pk}$, can be modeled as synchrotron radiation from a power-law distribution of electrons above $\gamma_{e,m}$ and do not couple to ALPs in our present study.

To explore photon-ALP mixing in the GRB jet environment, we solve the field evolution equation [Eq. (2.7)] with mixing matrix elements [Eq. (2.6)] derived from GRB environment parameters, and with initial electromagnetic field input from Eq. (3.1). Note that the comoving frame values for the GRB parameters are used to evaluate photon-ALP mixing, and the resulting effect show up in the comoving frame frequency ω. The observed photon energy is $E = \omega\Gamma/(1+z)$. We calculate the effect of photon-ALP mixing on the polarization pattern by using $A_\perp$ and $A_\parallel$ from solutions of the evolution equation [Eq. (2.7)] to find the linear degree of polarization as

$$\Pi_{L,{\rm ALP}} \equiv \frac{P_{\perp,{\rm ALP}}(\omega) - P_{\parallel,{\rm ALP}}(\omega)}{P_{\perp,{\rm ALP}}(\omega) + P_{\parallel,{\rm ALP}}(\omega)}\ , \tag{3.6}$$

and compare with Eq. (3.5), without photon-ALP mixing. We also define a flux modification factor, from Eq. (3.4), as

$$\rho = P(\omega)_{\rm ALP}/P(\omega)\ , \tag{3.7}$$

which shows any deviation from the synchrotron spectra due to photon-ALP mixing in the GRB jet. We discuss results from our investigation next.

4. Results and Discussion

For the nominal values of the GRB parameters $B_T = 10^6$ G, $n_e = 10^8$ cm^{-3}, $L = 10^{11}$ cm, and for the photon-ALP coupling constant $g_{a\gamma} = 8.8 \cdot 10^{-11}$ GeV^{-1} which is very close to the current CAST limit [7]; strong mixing of photons and ALPs takes place in the GRB jet when $m_a \leq \sqrt{2g_{a\gamma}\omega B_T} \lesssim 10^{-6}\sqrt{\omega/{\rm keV}}$ eV, from the condition $\Delta_a^2 \leq 4\Delta_{a\gamma}^2$. Indeed the photon-ALP mixing term $\Delta_{a\gamma}$ dominates other terms [Eq. (2.6)] in the mixing matrix for the nominal GRB parameters, and $\Delta_{\rm osc} \approx 2\Delta_{a\gamma} \sim L^{-1}$ [Eq. (2.8)]. The mixing angle θ is also maximized in this case, as $(\Delta_\parallel - \Delta_a) < \Delta_{a\gamma}$. The off-diagonal rotation term $\propto (\Delta_\parallel - \Delta_\perp) = (3/2)\Delta_{\rm QED} \sim 2\cdot 10^{-12}(\omega/{\rm keV})$ cm^{-1} is small at low ω for the nominal GRB parameters, but can become significant at high ω. Thus it is important to keep all terms in

[6] See e.g. Ref. [40] for power-law distribution of electron Lorentz factor.

the mixing matrix and solve the evolution equation [Eq. (2.3)] numerically with frequency-dependent initial conditions from Eq. (3.1). Photon-ALP conversion mostly takes place in a broad observed energy range of $E \approx (12\text{–}560)(\Gamma/100)(1+z)^{-1}$ keV [Eq. (2.9)] for our reference parameters.

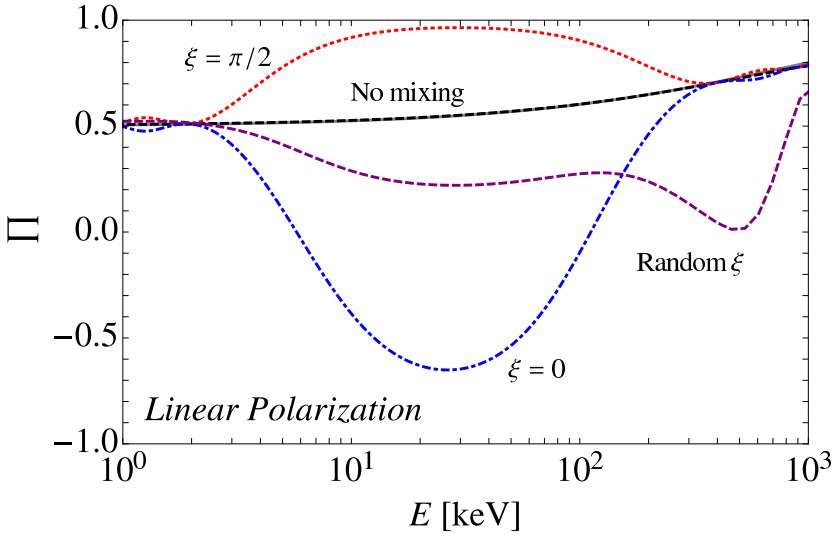

Figure 1: Linear photon polarization with and without ALP mixing in the GRB jet for the nominal GRB parameters $B_T = 10^6$ G, $n_e = 10^8$ cm^{-3} and $L = 10^{11}$ cm. We used a photon-ALP coupling parameter value $g_{a\gamma} = 8.8{\cdot}10^{-11}$ GeV^{-1} along with ALP mass $m_a = 10^{-7}$ eV. The GRB is assumed to be at redshift $z = 2$ with a jet bulk Lorentz factor $\Gamma = 100$. Also the synchrotron emission from the GRB is assumed to peak at ≈ 660 keV in the observer's frame. The polarization degree without photon-ALP mixing is shown as the black dashed line obtained by solving the evolution equation [Eq. (2.7)]. The solid gray line is the expected polarization from synchrotron theory. The role of the final $A_\parallel$ and $A_\perp$ are interchanged from the initial configuration while ξ changes from 0 (blue dot-dashed line) to $\pi/2$ (red dotted line). Total polarization from many identical domains but with random ξ is also shown (purple dashed line).

Figure 1 shows the effects of photon-ALP mixing in the GRB jet with nominal parameters as mentioned above with $\Gamma = 100$ and $z = 2$. The peak of the synchrotron radiation is assumed at $\omega_c = 20$ keV in the comoving GRB jet frame (2 MeV in the rest frame of the source or ≈ 660 keV in the observer's frame). The initial polarization obtained by numerically solving the evolution equation [Eq. (2.7)], without photon-ALP mixing, is plotted with the black dashed line, which agrees with theoretical expectation (solid gray line). The results for photon-ALP mixing are plotted for two cases, $\xi = 0$ (blue dot-dashed line) and $\xi = \pi/2$ (red dotted line). The change in polarization from the $\xi = 0$ case to the $\xi = \pi/2$ case can be understood as the magnetic field orientation in the initial production region and propagation region being aligned parallel with each other in the former case and being aligned perpendicular to each other in the latter case. In other words, as an inspection of the mixing matrix in Eq. (2.7) reveals, the $A_\parallel$ and $A_\perp$ in the final states are interchanged from the initial configuration for $\xi = \pi/2$. Observations in limited energy bands, however, can not distinguish between the two extreme cases and is expected to be intermediate, since

polarimeters measure the absolute degree of polarization, highly correlated with ξ within a unique energy band. On the other hand, a change in polarization degree in different energy bands, different from the synchrotron radiation pattern, can be used to search for photon-ALP mixing signature.

Time-resolved measurements over small intervals and around the pulses in the GRB light curves are important to ensure that emission from only a small bright spot, in which we assume the magnetic field to be fully coherent, of the jet surface contributes in each case. For longer exposure, contributions from many domains (assumed identical) on the jet surface can contribute. This case, where each domain is assumed to have completely ordered field within and only the orientation of the magnetic field direction ξ is assumed random, is also shown in Fig. 1 with the purple dashed line.

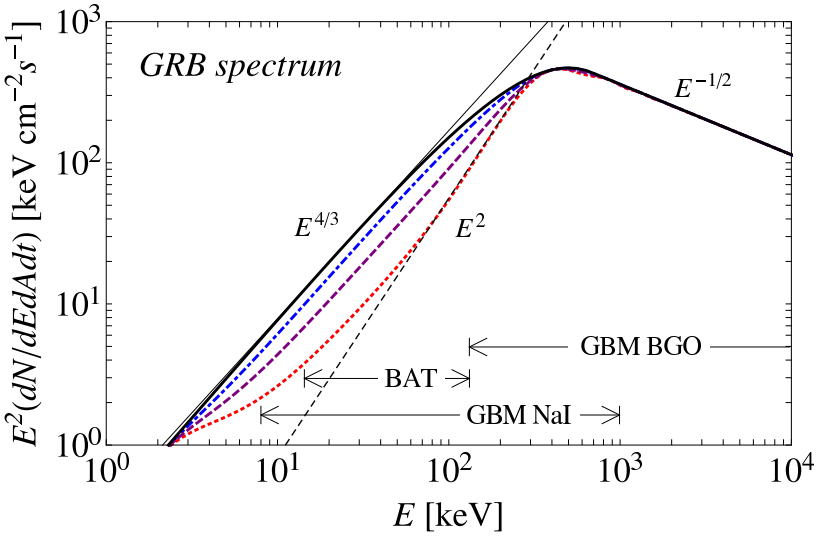

Figure 2: Phenomenological GRB energy spectrum with and without photon-ALP mixing with the same parameters used in Fig. 1. The spectrum for no photon-ALP mixing (solid thick black line) is plotted using the Band spectrum with peak photon energy $E_{\rm pk,Band} = 500$ keV, and low (high) energy power-law slope $\alpha_{\rm Band} \approx -0.6$ ($\beta_{\rm Band} = -5/2$). Asymptotically the low energy power-law slope coincides with the expected spectrum with $\alpha_\gamma = -2/3$ from synchrotron theory (thin solid gray line). The effects of photon-ALP mixing are plotted by multiplying the Band spectrum with the suppression factor in Eq. (3.7) for the $\xi = 0$ (blue dot-dashed line), $\xi = \pi/2$ (red dotted line) and random ξ (purple dashed line) cases. As can be seen, the observed spectra for the $\xi = \pi/2$ case can be steeper than the synchrotron spectrum in a limited energy range (thin dashed gray line). Also plotted are the energy bands in which *Swift* BAT and *Fermi* GBM instruments are sensitive.

Figure 2 shows the effects of photon-ALP mixing on the GRB spectrum. A phenomenological photon spectrum (dN/dE), called the Band spectrum [57], is plotted (thick black curve) with the low-energy index $\alpha_{\rm Band} \approx -0.6$, high energy power-law index $\beta_{\rm Band} = -5/2$ and a peak energy $E_{\rm pk,Band} = 500$ keV. The GRB is assumed to be at $z = 2$ as in Fig. 1 with all other parameters for photon-ALP mixing the same as those used for Fig. 1. We assume that synchrotron radiation from minimum energy electrons dominates below the start of the high energy power-law part of the spectrum at $(2+\alpha_{\rm Band})E_{\rm pk,Band} \approx 700$ keV,

similar to ω_c in the jet comoving frame. The effective low energy power-law index [51], corresponding to the synchrotron theory, is then $\alpha_\gamma \approx -2/3$ ($E^{4/3}$ in the E^2dN/dE or νF_ν spectrum) as plotted with a thin solid gray line. Approximately 20% of the GRB spectra are steeper than this "synchrotron death line", and in $\approx 5\%$ of the time-resolved spectra of bright GRBs the spectral deviation is statistically significant [50]. As shown in Fig. 2 photon-ALP mixing for $\xi = \pi/2$ case (red dotted line) can change the low-energy spectrum to as steep as $dN/dE \propto E^0$ (thin gray dashed line) from the synchrotron model, depending on the parameters we used. The change in the spectrum is not as significant, however, for the $\xi = 0$ and random ξ cases.

The $\xi = \pi/2$ case should be less frequent in nature as evidenced by the fraction of GRB spectra that violates the "synchrotron death line". High polarization degree, up to 100%, is expected in these cases (Fig. 1). Indeed the peak-resolved spectra of GRB 021206 with $(80 \pm 20)\%$ polarization [41] show low-energy index as hard as $\alpha_{\rm Band} = -0.42 \pm 0.05$ [58]. A larger sample of GRBs with correlated high polarization and steep low-energy spectrum detected with future polarimeters will be instrumental to probe the photon-ALP mixing in GRB jets. Other explanation of steep spectrum by black body, jitter radiation, inverse Compton scattering etc. (see e.g. Ref. [59]) do not generally change the polarization pattern the way photon-ALP mixing does and as we discussed here.

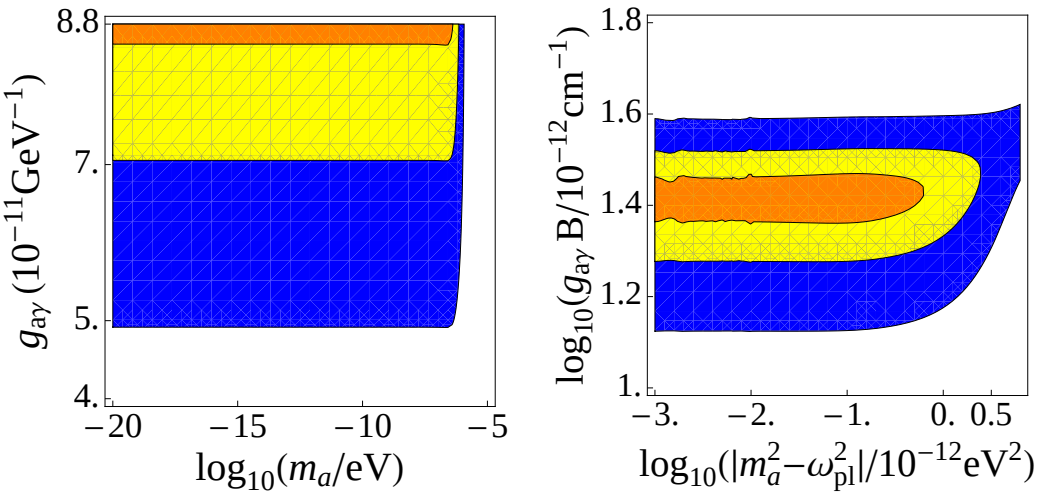

Figure 3: Contour plots of the flux suppression factor in the ALP parameter plane with fixed GRB parameters (left panel), and in the mixed ALP-GRB parameter plane (right panel). The outer, middle and inner contours depict the regions in which the flux suppression factor, see Eq. (3.7), reaches 70%, 50% and 40%, respectively. For $m_a < 10^{-6}$ eV, the effect becomes independent of the ALP mass and is restricted to a rather narrow range of $g_{a\gamma}B$ values.

Figure 3, left panel, depicts the flux suppression factor ρ, see Eq. (3.7), in the m_a–$g_{a\gamma}$ plane with fixed GRB parameters ($B_T = 10^6$ G, $n_e = 10^8$ cm^{-3} and $L = 10^{11}$ cm). The outer, middle and inner contours depict the regions in which the flux suppression factor reaches 70%, 50% and 40%, respectively.[7] The suppression effect has been averaged in the

[7] A smaller suppression factor corresponds to a larger conversion probability of photons to ALPs.

(10–500) keV energy window. A flux suppression factor $< 40\%$, requires a photon ALP coupling parameter close to the current CAST limit. As previously discussed, the mixing angle is maximized when the photon-ALP mixing term dominates the system evolution, and, for sufficiently small ALP masses ($m_a < 10^{-6}$ eV), the effect becomes independent of the ALP mass. In the pure axion cold dark matter (CDM) scenario, if the PQ symmetry is restored after inflation, a lower mass bound $m_a > 10^{-5}$ eV applies in order to not overclose the universe (see Ref. [60] and references therein). However, if inflation takes place after the PQ transition, much smaller values for the CDM axion mass are still allowed, see Refs. [61, 62, 63, 64]. The ALP case is more complicated, since these particles constitute a dark matter candidate only under certain conditions. For instance, if ALPs couple exclusively to photons, they are excluded as CDM candidates [65]. Consequently, no lower ALP mass bound is shown in Fig. 3 (left panel), since the role of ALPs as CDM particles depends highly on the underlying theoretical model.

Figure 3, right panel, depicts the flux suppression factor ρ same as in the left panel. The contours are plotted in the $g_{a\gamma}B$ and $|m_a^2 - \omega_{\rm pl}^2|$ plane, where both the quantities are closely related to the wave numbers [Eq. (2.6)]. Comparing the ranges of $g_{a\gamma}$ and $g_{a\gamma}B$ values from the plots, significant ($\lesssim 70\%$) flux suppression takes place for $B \sim 4 \cdot 10^5$–$3 \cdot 10^6$ G in the observed keV–MeV range. Thus detection of photon-ALP mixing effect in GRB data can, in principle, be used to probe the magnetic field value in the GRB jet, which is somewhat uncertain. Note that a much higher, $\sim 10^9$ G, field with a $\sim 10^6$ cm coherence length, corresponding to the neutron star radius used in Refs. [31, 32] gives no photon-ALP mixing effect in the GRB jet. However, the radius of γ-ray emission region is likely to be large to avoid e^+e^- pair creations by the photons and thermalization. The magnetic field in the jet is thus likely to be small, typical to the values that we used, at this large radius.

Mixing of photons with ALPs, for propagation in the IGMF with generally assumed magnetic field $B_{\rm IGMF} = 1$ nG and particle density $n_e = 10^{-7}$ cm^{-3}, takes place in the frequency range [see Eq. (2.9)] $\omega_L \approx 10^7 (m_a/10^{-7}\ {\rm eV})^2 (B_{\rm IGMF}/{\rm nG})^{-1}$ GeV and $\omega_H \approx 6 \cdot 10^9 (B_{\rm IGMF}/{\rm nG})^{-1}$ GeV for the same $g_{a\gamma}$ parameter from the CAST limit. The contribution of plasma frequency to ω_L becomes dominant for ALP mass $m_a \ll 10^{-14}\sqrt{n_e/10^{-7}\ {\rm cm}^{-3}}$ eV from the condition $\omega_{\rm pl} \gg m_a$ in Eq. (2.9). The corresponding $\omega_L \approx 0.1 (n_e/10^{-7}\ {\rm cm}^{-3})(B_{\rm IGMF}/{\rm nG})^{-1}$ keV becomes constant. The oscillation wave number is $\Delta_{\rm osc} \approx \Delta_{a\gamma}$ in this asymptotic range, and the oscillation probability [Eq. (2.8)] is $P_{a\gamma} \approx (\Delta_{a\gamma} L)^2 \approx 2 \cdot 10^{-3} (B_{\rm IGMF}/{\rm nG})^2 (L/{\rm Mpc})^2$ for Mpc scale coherence length. Thus photon-ALP mixing in the IGMF can be important over Gpc scale source distance and wash-out the source signature only if the IGMF is of the order of nG and the ALP mass is smaller than 10^{-14} eV. This result is compatible with mixing effect in the IGMF for ultra-light ALPs explored in Ref. [32]. In fact these two mixing scenarios, in-source and in the IGMF, are complementary to each other and cover a huge range of ALP mass. Detection of source signatures can be used to constrain the ALP mass as well as to put limit on the IGMF. Indeed, there are hints from recent studies of ultra high-energy cosmic ray data and TeV blazars that the IGMF can be much smaller than a nG [66], in which case the polarization and spectral signatures of in-source photon-ALP mixing that we explored

will not be destroyed. Photon-ALP mixing in the $\sim \mu$G galactic magnetic field over kpc coherence length scale is also negligible.

5. Conclusions

Axions and axion-like particles appear in many extentions of the standard model of particle physics. Photon-axion/ALP mixing in the presence of an external electromagnetic field constitutes one of the most exploited signals for astrophysical and laboratory axion and ALP searches. Gamma-ray bursts are the most powerful source of keV–MeV photons in nature, which are most probably synchrotron radiation. These photons originate and propagate inside the GRB jet with high magnetic field. We have shown that strong photon-ALP conversion takes place in GRB jet in the ~ 100 keV observed energy range, distorting the standard synchrotron polarization pattern. We have also shown that when the magnetic field direction in the photon propagation coherence length is perpendicular to the magnetic field direction in the synchrotron radiating region, the photon energy spectrum will be steeper than the expected spectrum from synchrotron theory, thus providing an explanation for the anomalous spectra of $\sim 20\%$ of the observed GRBs. We found that the photon-ALP conversion occurs within a large range of possible GRB and ALP parameters, being almost independent of the ALP mass for sufficiently small ALP masses ($m_a < 10^{-6}$ eV). Further modification due to mixing in the intergalactic magnetic field is not expected in case the IGMF is $\lesssim 1$ nG and/or the ALP mass is $\gtrsim 10^{-14}$ eV.

Large statistics expected to be collected by a number of future missions that are devoted to measure GRB polarization in the keV–MeV range will be crucial to search for ALP signals due to their mixing with photons inside GRBs.

6. Acknowledgments

We thank Mikhail Medvedev, Carlos Peña-Garay, John Ralston and Kenji Toma for helpful discussions, and Justin Finke for useful comments on the manuscript. Work of O. M. was supported by the MICINN (Spain) Ramón y Cajal contract, AYA2008-03531 and CSD2007-00060. Work of S. R. was performed at and under the sponsorship of the Naval Research Laboratory (USA) and was partially supported by the Fermi Cycle 2 Guest Investigator Program of NASA (USA).

References

[1] R. D. Peccei and H. R. Quinn, Phys. Rev. Lett. **38**, 1440 (1977); R. D. Peccei and H. R. Quinn, Phys. Rev. D **16**, 1791 (1977).

[2] S. Weinberg, Phys. Rev. Lett. **40**, 223 (1978).

[3] F. Wilczek, Phys. Rev. Lett. **40**, 279 (1978).

[4] G. Raffelt and L. Stodolsky, Phys. Rev. D **37**, 1237 (1988).

[5] M. S. Turner, Phys. Rev. Lett. **59**, 2489 (1987) [Erratum-ibid. **60**, 1101 (1988)].

[6] E. W. Kolb and M. S. Turner, *"The Early Universe"*, Addison Wesley (1990).

[7] S. Andriamonje *et al.* [CAST Collaboration], JCAP **0702**, 010 (2007) [arXiv:hep-ex/0702006].

[8] L. D. Duffy *et al.*, Phys. Rev. D **74**, 012006 (2006) [arXiv:astro-ph/0603108].

[9] C. Csaki, N. Kaloper and J. Terning, Phys. Rev. Lett. **88** (2002) 161302 [arXiv:hep-ph/0111311]. C. Csaki, N. Kaloper and J. Terning, Phys. Lett. B **535**, 33 (2002) [arXiv:hep-ph/0112212].

[10] C. Deffayet, D. Harari, J. P. Uzan and M. Zaldarriaga, Phys. Rev. D **66**, 043517 (2002) [arXiv:hep-ph/0112118].

[11] L. Ostman and E. Mortsell, JCAP **0502**, 005 (2005) [arXiv:astro-ph/0410501].

[12] B. A. Bassett, Astrophys. J. **607**, 661 (2004) [arXiv:astro-ph/0311495].

[13] A. Mirizzi, G. G. Raffelt and P. D. Serpico, Phys. Rev. D **72** (2005) 023501 [arXiv:astro-ph/0506078]. A. Mirizzi, G. G. Raffelt and P. D. Serpico, Phys. Rev. D **72** (2005) 023501 [arXiv:astro-ph/0506078].

[14] A. Avgoustidis, C. Burrage, J. Redondo, L. Verde and R. Jimenez, arXiv:1004.2053 [astro-ph.CO].

[15] N. Agarwal, P. Jain, D. W. McKay and J. P. Ralston, Phys. Rev. D **78**, 085028 (2008) [arXiv:0807.4587 [hep-ph]].

[16] C. Csaki, N. Kaloper, M. Peloso and J. Terning, JCAP **0305** (2003) 005 [arXiv:hep-ph/0302030].

[17] A. Mirizzi, G. G. Raffelt and P. D. Serpico, Phys. Rev. D **76**, 023001 (2007) [arXiv:0704.3044 [astro-ph]].

[18] M. A. Sanchez-Conde, D. Paneque, E. Bloom, F. Prada and A. Dominguez, Phys. Rev. D **79**, 123511 (2009) [arXiv:0905.3270 [astro-ph.CO]].

[19] A. De Angelis, O. Mansutti and M. Roncadelli, Phys. Lett. B **659** (2008) 847 [arXiv:0707.2695 [astro-ph]].

[20] N. Bassan and M. Roncadelli, arXiv:0905.3752 [astro-ph.HE].

[21] S. Razzaque, C. D. Dermer and J. D. Finke, Astrophys. J. **697**, 483 (2009) [arXiv:0807.4294 [astro-ph]].

[22] A. Loeb, Phys. Rev. D **48**, 3419 (1993) [arXiv:astro-ph/9308048].

[23] O. Bertolami, Astropart. Phys. **11**, 357 (1999) [arXiv:astro-ph/9901184].

[24] Z. Berezhiani and A. Drago, Phys. Lett. B **473**, 281 (2000) [arXiv:hep-ph/9911333].

[25] C. A. Meegan *et al.*, Nature **355**, 143 (1992).

[26] F. W. Stecker, M. A. Malkan and S. T. Scully, Astrophys. J. **648** (2006) 774 [arXiv:astro-ph/0510449].

[27] T. M. Kneiske, T. Bretz, K. Mannheim and D. H. Hartmann, Astron. Astrophys. **413**, 807 (2004) [arXiv:astro-ph/0309141].

[28] A. Franceschini, G. Rodighiero and M. Vaccari, arXiv:0805.1841 [astro-ph].

[29] R. C. Gilmore, P. Madau, J. R. Primack, R. S. Somerville and F. Haardt, arXiv:0905.1144 [astro-ph.CO].

[30] J. D. Finke, S. Razzaque and C. D. Dermer, Astrophys. J. **712** (2010) 238 [arXiv:0905.1115 [astro-ph.HE]].

[31] A. Rubbia and A. S. Sakharov, Astropart. Phys. **29**, 20 (2008) [arXiv:0708.2646 [hep-ph]].

[32] N. Bassan, A. Mirizzi and M. Roncadelli, JCAP **1005** (2010) 010 [arXiv:1001.5267 [astro-ph.HE]].

[33] C. Burrage, A. C. Davis and D. J. Shaw, Phys. Rev. D **79**, 044028 (2009) [arXiv:0809.1763 [astro-ph]].

[34] H. C. Spruit, F. Daigne and G. Drenkhahn, Astron. Astrophys. **369**, 694 (2001) [arXiv:astro-ph/0004274].

[35] M. Lyutikov, V. I. Pariev and R. D. Blandford, Astrophys. J. **597**, 998 (2003) [arXiv:astro-ph/0305410].

[36] M. J. Rees and P. Meszaros, Astrophys. J. **430**, L93 (1994) [arXiv:astro-ph/9404038].

[37] J. I. Katz, Astrophys. J. **432**, L107 (1994) [arXiv:astro-ph/9312034].

[38] M. Tavani, Astrophys. J. **466**, 768 (1996).

[39] M. V. Medvedev and A. Loeb, Astrophys. J. **526**, 697 (1999) [arXiv:astro-ph/9904363].

[40] G. B. Rybicki and A. P. Lightman, "Radiative Processes in Astrophysics," New York: Wiley, 179 (1979).

[41] W. Coburn and S. E. Boggs, Nature **423**, 415 (2003) [arXiv:astro-ph/0305377].

[42] R. E. Rutledge and D. B. Fox, Mon. Not. Roy. Astron. Soc. **350**, 1272 (2004) [arXiv:astro-ph/0310385].

[43] D. Yonetoku *et al.*, arXiv:1010.5305 [astro-ph.IM].

[44] S. E. Boggs *et al.*, NASA Vision Mission Concept Study Report, [arXiv:astr0-ph/0608532].

[45] J. Greiner *et al.*, Experimental Astronomy **23**, 91 (2009).

[46] J. E. Hill *et al.*, AIP Conf. Proc. **1065**, 331 (2008) [arXiv:0810.2499 [astro-ph]].

[47] K. Toma *et al.*, Astrophys. J. **698**, 1042 (2009) [arXiv:0812.2483 [astro-ph]].

[48] J. D. Jackson, "Classical Electrodynamics," New York: Wiley, 679 (1998).

[49] R. Sari, T. Piran and R. Narayan, Astrophys. J. **497**, L17 (1998) [arXiv:astro-ph/9712005].

[50] Y. Kaneko, R. D. Preece, M. S. Briggs, W. S. Paciesas, C. A. Meegan and D. L. Band, Astrophys. J. Supp. **166**, 298 (2006) [arXiv:astro-ph/0605427].

[51] R. D. Preece, M. S. Briggs, R. S. Mallozzi, G. N. Pendleton, W. S. Paciesas and D. L. Band, Astrophys. J. **506**, L23 (1998) [arXiv:astro-ph/9808184].

[52] H. A. Krimm *et al.*, Astrophys. J. **704**, 1405 (2009) [arXiv:0908.1335 [astro-ph.HE]].

[53] G. Ghirlanda, L. Nava and G. Ghisellini, Astron. Astrophys. **511**, A43+ (2010) arXiv:0908.2807 [astro-ph.HE].

[54] A. Gruzinov and E. Waxman, Astrophys. J. **511**, 852 (1999) [arXiv:astro-ph/9807111].

[55] S. Razzaque, P. Meszaros and B. Zhang, Astrophys. J. **613**, 1072 (2004) [arXiv:astro-ph/0404076].

[56] J. Granot and A. Königl, Astrophys. J. **594**, L83 (2003)

[57] D. Band *et al.*, Astrophys. J. **413**, 281 (1993)

[58] C. Wigger, O. Wigger, E. Bellm and W. Hajdas, Astrophys. J. **675**, 553 (2008) arXiv:0710.2858 [astro-ph].

[59] G. Ghirlanda, A. Celotti and G. Ghisellini, Astron. Astrophys. **406**, 879 (2003)

[60] K. Nakamura et al. (Particle Data Group), J. Phys. G 37, 075021 (2010)

[61] A. D. Linde, Phys. Lett. B **201**, 437 (1988).

[62] M. Tegmark, A. Aguirre, M. Rees and F. Wilczek, Phys. Rev. D **73**, 023505 (2006) [arXiv:astro-ph/0511774].

[63] A. Arvanitaki, S. Dimopoulos, S. Dubovsky, N. Kaloper and J. March-Russell, Phys. Rev. D **81**, 123530 (2010) [arXiv:0905.4720 [hep-th]].

[64] L. Visinelli and P. Gondolo, Phys. Rev. D **80**, 035024 (2009) [arXiv:0903.4377 [astro-ph.CO]].

[65] E. Masso, Lect. Notes Phys. **741**, 83 (2008) [arXiv:hep-ph/0607215].

[66] A. Neronov and I. Vovk, Science **328**, 73 (2010); F. Tavecchio, G. Ghisellini, L. Foschini, G. Bonnoli, G. Ghirlanda and P. Coppi, Mon. Not. R. Astron. Soc. **406**, L70 (2010); S. Ando and A. Kusenko, Astrophys. J. **722**, L39 (2010); C. D. Dermer, M. Cavadini, S. Razzaque, J. D. Finke, and B. Lott, arXiv:1011.6660 (submitted to ApJL).